Index UDC: 621.3

Development of a Hybrid Energy Recovery System within Power Grid

Feng Yang, Lin Du

***Abstract*—This paper focuses on utilizing potential energy resources within power grid and developing a novel approach to provide power supply for sensor application by using the recovered energy. To this end, the paper has investigated methods of magnetic, thermoelectric and vibration energy recovery from power equipments in substations, and developed a hybrid energy management system. When combined, the three energy conversion devices can produce enough output electricity to drive the load. Performance of three energy recovery approaches has been assessed first regarding their converted power capacity and output properties. Whereafter simulation and experiments on power conversion and hybrid management circuit have been applied. It indicates that in situations of representative ambient energy profiles, magnetic and thermoelectric harvesters can output 366mW and 1.98W, while vibration transducer outputs 0.63mW. Tentative application reveals that the energy recovery methodology involved is feasible and converted electricity is usable for some low-power sensors. Finally, the paper has characterized an envisioned prototype for energy recovery with sensors embedded. The scheme may also provide indications to other large-scale industrial energy recovery deployment.**

***Index Terms*—Energy recovery, power grid, magnetic, thermoelectric, vibration, hybrid energy management**

I. Introduction

Energy use around the world is rising drastically. The total world energy use is expected to rise from 505 quadrillion British thermal units (Btu) in 2008 to 619 quadrillion Btu in 2020 and 770 quadrillion Btu in 2035 [1]. Fossil fuels, including liquid fuels, natural gas, and coal, are expected to supply approximately 80% of the world's energy need in 2035. As a result, the world's energy-related carbon dioxide emission is expected to increase from 30.2 billion metric tons in 2008 to 43.2 billion metric tons in 2035. The worldwide intensifying energy crisis and greenhouse effect are demanding to be retarded. Renewable and alternative energy sources can assist in reducing use of fossil fuels and greenhouse gas emissions [2]. On the other hand, improving energy consumption efficiency and recovering waste power from industries and household are equally significant [3].

F. Yang and L. Du are now with State Key Laboratory of Power Transmission Equipment & System Security and New Technology, Chongqing University, Chongqing 400044, China. (e-mail: yangfeng@cqu.edu.cn; dulin@cqu.edu.cn, tel: +86 153-1027-0139; +86 138-9606-1868).

Regarding power grid, it converts various kinds of primary energy (e.g. fossil, hydroelectric, nuclear, wind, solar) and distributes electricity to end users. However, there is notable energy wasted during operation of the grid. For instance, according to the data released in 2014 by National Energy Administration of China, the domestic installed capacity of the power system has reached 1.3 billion kW. Usually there will be approximately 1.6% of total capacity being exhausted in the form of heat from transformer [4]. This means that at least 20 million kW of electricity power is dissipated per year. The figure indicates a case of remarkable power waste while China is undergoing energy intension with increasing economic development of late years [5].

Except the desire of energy saving, another motivation of the paper is to find alternative power supply for condition monitoring sensors of power equipments. It's a longstanding problem that in some occasions, conventional power source for sensors may be unavailable within power grid, like for those sensors mounted in HV ends [6]. With the development of emerging energy harvesting technologies, attempts to power sensors with recovered energy from ambient seem to be applicable.

Energy harvesting or energy recovery means scavenging various form of energy from ambient [7]. And there are multiple location dependent energy resources for sensors in power grid, including solar, thermal, vibration, wind, and electromagnetic energy [8]. Among them, magnetic, thermoelectric and vibration energy have more opportunity to be recovered, due to their undisputed abundance under power grid environment, which are directly affiliated to three prominent effects of current, i.e., calorific effect, electrodynamics effect and electromagnetic induction. Their presence underlies the implementation of recovering the three potential energy resources. Nevertheless, three recovered energy is of intermittent and low power level essence, risking power shortage or outrages. Accordingly, the paper also investigated hybrid architecture for multiple energy sources. The rest of the paper is organized as follows. Section II details the principles, properties and implementation of three energy recovery methods by simulation and experiments. Section III introduces the structure and performance of hybrid energy management system and demonstrates the application with sensor load. Section IV characterizes a kind of envisioned prototype for energy recovery with embedded sensors. And section V concludes the paper.

II. Energy Recovery Methods

A. Magnetic Energy Recovery

Magnetic energy is abundant within power grid, especially in substations or near transmission lines. Magnetic field excited by high current can be harvested by coil and windings in the manner of electromagnetic induction. In order to understand magnetic energy distribution under power grid environment, theoretical analysis and assessment are presented.

The magnetic field around a segment of 35kV bus bar bridge (Fig.1) in a 220kV substation was selected to be analyzed. Referenced to *Typical Design for Power Transmission and Transformation Project of State Grid Corporation: Fascicule of 220kV Substation* [9] and *GBJ149—90 Erection Works of Electrical Installations Code for Construction and Acceptance of Bus-bar Device* [10], the type of bus bar was selected as LMY-125×10. And the length of the bus bar was set as 11m calculated from ichnography of typical design in [9]. The interphase distance and height were set as 0.4m and 2.9m (Fig.2). And the symmetric currents of three phase in the bus bar were set as 1039A, which are standard operation current of 35kV line in substations.

Fig. 1. 35kV bus bar bridge selected for analysis

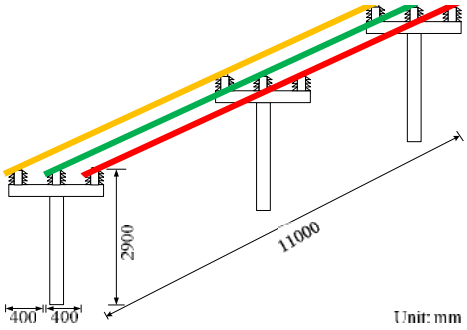

Fig. 2. Dimensions of the bus bar bridge set for calculation

Fig. 3. Calculation model of magnetic field

The calculation model of magnetic field is illustrated by Fig. 3. The coordinate system is placed along the rectangle bus bar. Magnetic induction intensity excited by each phase along x and y direction as well as total magnitude can be calculated as follows,

$$B_x = -\iint_{S_1} \frac{\mu_0 j}{4\pi\rho}\left[\frac{z}{\sqrt{\rho^2+z^2}} + \frac{L-z}{\sqrt{\rho^2+(L-z)^2}}\right]\frac{y-y_q}{\rho}\,dx_S dy_S \quad (1)$$

$$B_y = \iint_{S_1} \frac{\mu_0 j}{4\pi\rho}\left[\frac{z}{\sqrt{\rho^2+z^2}} + \frac{L-z}{\sqrt{\rho^2+(L-z)^2}}\right]\frac{x-x_q}{\rho}\,dx_S dy_S \quad (2)$$

$$B = \sqrt{B_x^2 + B_y^2} \quad (3)$$

where, x, y, z are coordinates of points in field; x_s, y_s are coordinates of points in source area; $\rho=[(x-x_s)^2+(y-y_s)^2]^{1/2}$; j means current density, that $j=I/(ab)$.

By Matlab programming, the distribution of amplitude of B value around bus bar is obtained as Fig. 4. Fig.5 is the components of B on x direction. B_x is critical to be identified as it's directly connected with the quantity of flux through energy harvesting core and winding.

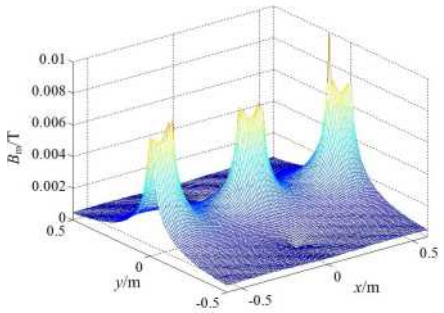

Fig. 4. Distribution diagram of B_m

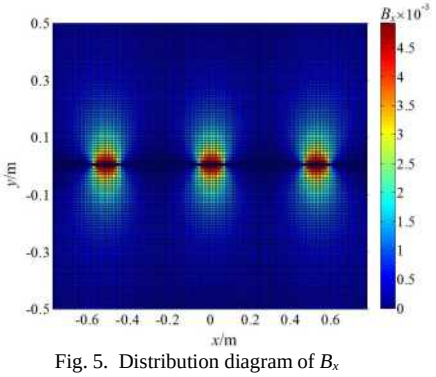

Fig. 5. Distribution diagram of B_x

Fig.4 and Fig.5 reveal that the magnetic field is intensive near the surface of bus bar and decays dramatically with the distance away from bus bar increased. The highest strength of B is 5×10^{-3}T. Understanding distribution of B, the magnetic energy harvester should be stick onto the surface in order to obtain the most intensive energy. Referenced to Fig.5, the area of intensive B_x locates underneath bus bar coverage

of three phases along *x* direction and [-0.1 m, 0.1 m] along *y* direction, which means the harvester should be installed within this area.

Conventional CT based structure is normally employed to draw out magnetic energy excited by conductors [11]. However, the whole set of devices are clamped around overhead bus bar or transmission line. It may lead to power outrages as required in its field installation. Besides, great proportion of iron core within the structure tends to increase its overall weight, which may threat long-term mechanical strengthen of overhead lines. Even in some occasions where three phases are arranged compactly, there is insufficient space left for iron ring, if specified interphase safety distance requirement is to be satisfied.

The paper presents a novel type of stick-on structure for magnetic energy recovery, shown in Fig.6. The appliance is possible to be stuck onto any utility asset where magnetic field is distributed. A special butterfly shaped iron core has been adopted, which has greater surface area at two ends, being critical to concentrate flux lines effectively. And for considerations of easy installation and maintenance, the hanging iron core and winding are fastened in a self-clamping manner, where permanent magnet is placed on the upper side of bus bar, generating magnetism acted on iron core and clamping them from two sides of the bus bar.

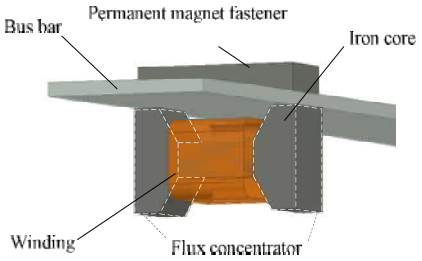

Fig. 6. Structure of magnetic energy harvester

The designed structure was simulated by Ansoft first in order to compare it with conventional core bar and hollow winding without iron core. The current in bus bar is set as 500A and *B* value were inspected, within the area of the same section along longitudinal axis of the three types of structures mentioned.

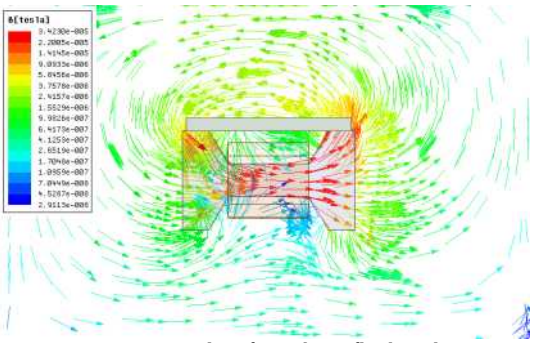

Fig. 7 Vector overlay of *B* on butterfly shaped core

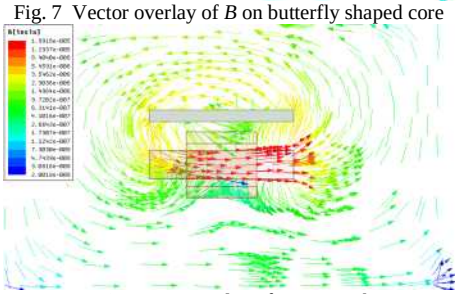

Fig. 8 Vector overlay of *B* on core bar

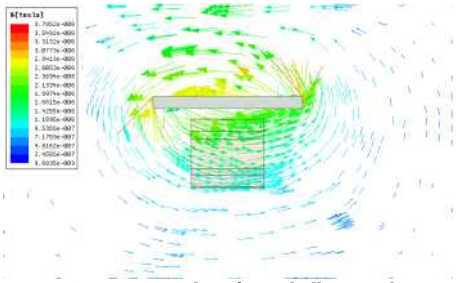

Fig. 9 Vector overlay of *B* on hollow winding

Fig.7, 8 and 9 reveal that presence of iron core will remarkly intensify *B* within its covered space, where the maximum of *B* has been increase by 426% with core bar. Designed butterfly shaped core was proved to be capable of concentrating flux, where maximum of *B* has been increase by 71.2% compared with the core bar. Efforts to concentrate flux is primary to optimize the output power as less turns can be wired to satisfly a specified minimum EMF, manwhile reduces inner resistance of wires, leading to greater output power capacity.

An optimization is needed, in order to search for the most appropriate dimensions of core and winding turns. Specifically, the peak power consumption of load should be covered. Whereafter the output capacity still needed to be maximized, offering sufficient power margin. Similarly, the total weight needed to be minimized within the range magnetism can uphold. These two considerations constitute optimization objectives. Constrain is that output voltage should match the operation voltage range specified by load, and spatial expanding of the body should not go beyond certain limits. To address this issue, a multiobjective

optimization model is adopted as (4), together with dimension illustration in Fig.10,

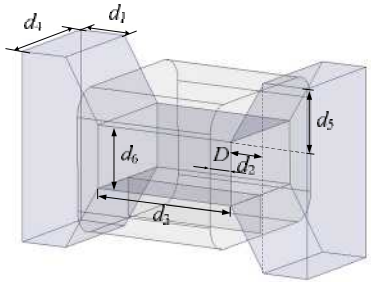

Fig. 10 Dimensions of iron core and winding

$$\begin{aligned} &\max\ P_{\max} = U^2/(4R_{\text{in}}) \\ &\min\ m = \rho V \\ &s.t.\ d_{n\text{MIN}} \le d_n \le d_{n\text{MAX}} \\ &D_{\text{MIN}} \le D \le D_{\text{MAX}} \\ &2(d_1 + d_2) + d_3 \le W \\ &2d_5 + d_6 \le H \\ &U_{\text{MIN}} \le U \le U_{\text{MAX}} \\ &P_{\max} \ge P_{\text{MAX}} \end{aligned} \tag{4}$$

where $U=f_1(d_n,D)$, $R_{in}=f_2(d_4,d_6,D)$, $V=f_3(d_n)$. U denotes output voltage of the core and R_{in} denotes inner resistance of winding. W and H denote width and height limit of the core. D means thickness of the winding. V means volume of the core and ρ means density of the iron core. U_{MIN}, U_{MAX} and P_{MAX} denote the two voltage threshold values and maximum power consumption of the load. These limitation values were set in accordance with the sensor load which will be adopted in tentative application in Section III.

The optimization (4) can be solved with Sequential Mixed Integer Nonlinear Programming, performed by Maxwell's Optimetrics toolbox. If target value in searching converges within given maximum iterations, the optimal dimensions of the core are identified, as showed in Fig.11.

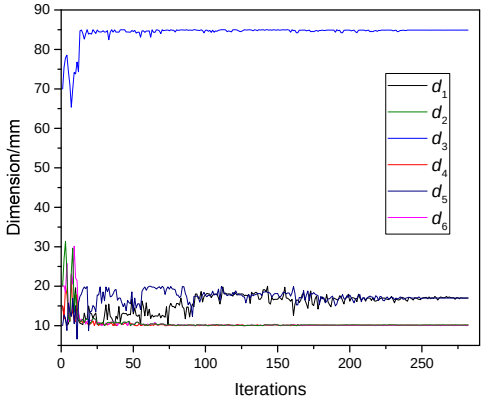

Fig. 11. Convergence of core dimension

If G-53 wire is adopted, with 1mm diameter, and according to the optimization result, 100 turns are determined to be winded on the core. With the harvester, when in the current range of 100A to 800A on the bus bar, the maximum output power can be 0.7mW to 366mW, see Fig.12.

B. Thermoelectric Energy Recovery

It's reported that on a 63MVA transformer, high temperature is generally found at the center of the tank and in the upper part of the radiator ranging from 333 to 353K [12]. Assuming ambient air temperature to be 25□

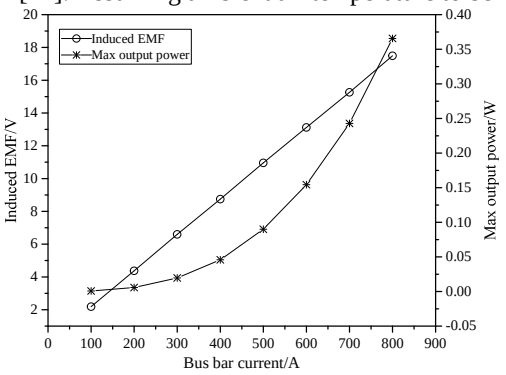

Fig. 12 Induced EMF & max output power vs. bus bar current

(298K), this leads to temperature difference of almost 55K. High temperature points on certain power equipments or transmission line are able to active thermoelectric generator (TEG).

The open circuit voltage of TEG can be given by [13], as

$$V_{oc}=2\alpha\Delta T_{TEG} \tag{5}$$

where, □α□denotes Seebeck coefficient and□ΔT_{TEG} denotes temperature gradient between hot and cold sides of TEG. Referring to Fig.14, heat transfer can be simulated by the circuit [14]. It indicates the output power can be optimized with the following three considerations: appropriate thermal arrangement for maximized ΔT_{TEG}; improved thermal properties of material with greater Seebeck coefficient α for higher V_{oc}; load impedance match, $R_{TEG}=R_L$.

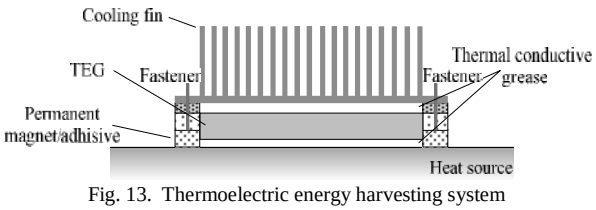

Fig. 13. Thermoelectric energy harvesting system

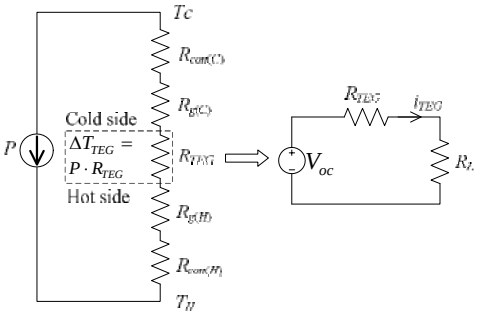

Fig. 14. Simulated circuit of thermal energy harvesting system.

Inside TEG, "p" and "n" type semiconductor materials constitute thermocouple. The electrical-thermal coupling within it can be expressed by following governing equations [15],

$$\boldsymbol{j} = \sigma \boldsymbol{E} - \sigma\alpha\nabla T \tag{6}$$

$$\boldsymbol{q} = \pi \boldsymbol{j} - k\nabla T \tag{7}$$

$$\boldsymbol{E} = -\nabla\left(\frac{\mu}{-e} + \varphi\right) \tag{8}$$

Where:

σ = electrical conductively, S/m,
α = Seebeck coefficient, V/K,
π = Peltier coefficient, V,
μ = Fermi level, eV,
φ = potential, V,
k = thermal conductivity, W/(m·K),
$\boldsymbol{j}$ = current density vector, A/m^2,
$\boldsymbol{E}$=electric field intensity vector, V/m,
$\boldsymbol{q}$= heat flux vector, W/m^2.

Distribution of temperature can be identified as solution of equations involving (6)-(8), under following steady-state condition,

$$\{\mathrm{div}(\boldsymbol{j}) = 0, \mathrm{div}(\boldsymbol{w}) = 0\} \tag{9}$$

where, w means total energy flux density that

$$\boldsymbol{w} = \left(\boldsymbol{q} + \frac{\mu}{-e}\boldsymbol{j}\right) \tag{10}$$

The paper constructed an overall model of thermal energy recovery, specially taken in a segment of current-carrying bus bar as the heat source in order to exam thermal energy profile around it, also for the sake of investigating its application on bus bar. The model was solved using finite element analysis (FEA) method, by thermal-electric module in ANSYS Workbench, outputting graphical results as follows.

The whole simulation model (Fig.15) was computed by thermal-electric module in ANSYS Workbench. The current in bus bar was adjustable and temperature of ambient air is set as 25℃. Parametric analysis provides output characteristics of load dependence of operation voltage and output power, with current of 100A-600A on bus bar, which is considered to be most important properties if the system is to be housed on any current carrying conductors in power grid.

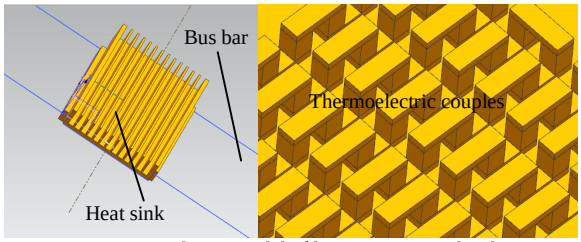

Fig. 15. Simulation model of heat recovery on bus bar

The model was solved using FEA method, by thermal-electric module in ANSYS Workbench, outputting graphical results as follows.

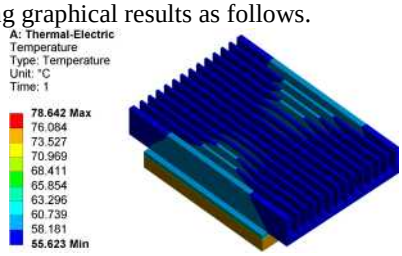

Fig. 16. Temperature gradient on thermoelectric energy recovery system

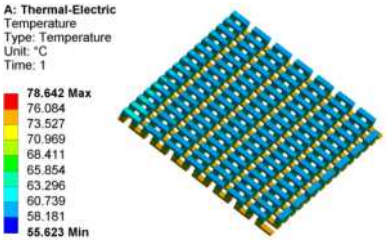

Fig. 17. Temperature gradient on thermoelectric

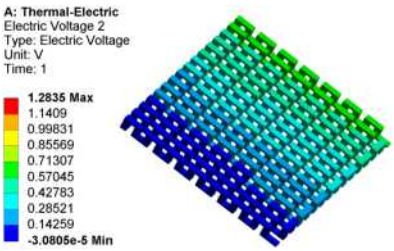

Fig. 18. Voltage distribution on thermoelectric couples

It brings about effective temperature gradient of 13.35℃ on two legs of thermocouple, which counts up 66.7% among total gradient, see Fig.16 and Fig.17. In this case, Fig.18 shows potential distribution and the output voltage of a single module reaches 0.64V. Parametric analysis provides dependence of open circuit voltage and output power on temperature gradient led by bus bar current from 500A to 2000A, see Fig. 19. It reveals that maximum output power increases as the current rises. Within considered range from 500A to

2000A, the maximum operational power of TEG ranges from 12.9mW to 1.98W.

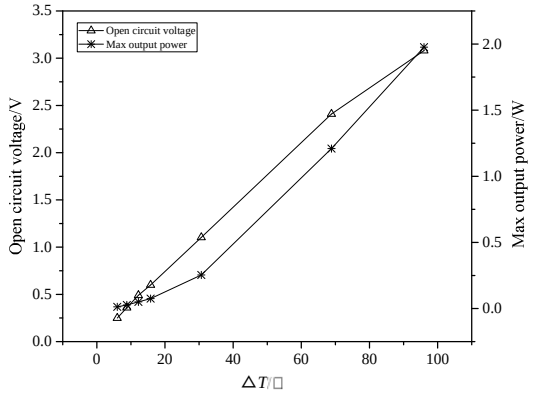

Fig. 19. Output power vs. temperature gradient

C. Vibration Energy Recovery

Untapped kinetic energy is almost everywhere in municipal infrastructures, automobiles and industrial plants. Also, it's plentiful in power plant and substations, which can be converted into electricity by means of transducers. Data from a recent study shows that the vibration level of an in-service 132/66 kV, 40 MVA transformer is above 1.0m/s^2 for most of the time, see measured curve of vibration acceleration in a transformer [16].

Recovery of vibration energy is mostly implemented by piezoelectric transducer (PZT). Bimorph type is usually adopted. From the perspective of fabrication, bimorph structure consists of piezoelectric material, PVDF, bonded onto upper and lower surfaces of conductive substrate, which also provides enough stiffness. Rectangular slice of bimorph is clamped at one end and free on the other, known as cantilever structure in Fig.20.

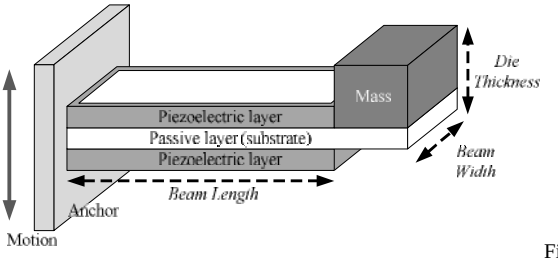

Fig.20. Structure of cantilever type piezoelectric harvesters

With reference of experimentally validated model in [17], bimorph motion is governed by the following equation,

$$\frac{\mathrm{d}^2\eta_r^s(t)}{\mathrm{d}t^2}+2\zeta_r\omega_r\frac{\mathrm{d}\eta_r^s(t)}{\mathrm{d}t}+\omega_r^2\eta_r^s(t)+\chi_r^sU(t)=-\frac{M_b}{L}\frac{\mathrm{d}^2y(t)}{\mathrm{d}t^2}\int_0^L\Phi_r(x)\mathrm{d}x-M_t\Phi_r(L)\frac{\mathrm{d}^2y(t)}{\mathrm{d}t^2} \quad (11)$$

where η_r^s is response of model under rth mode of bimorph vibration; ζ_r is its damping coefficient; ω_r is undamped natural angular frequency; χ_r^s is electromagnetic coupling term; M_b and L are mass and length of the beam; $\Phi_r(x)$ is model shape; M_t is mass attached onto the beam. The equation of electrical system can be written as,

$$\frac{C_p}{a}\frac{\mathrm{d}U(t)}{\mathrm{d}t}+\frac{aU(t)}{2R_L}=i_p(t)=k_r\frac{\mathrm{d}\eta_r^s(t)}{\mathrm{d}t} \quad (12)$$

Where

$$k_r=\frac{d_{31}h_{pc}b}{s_{11}^E}\frac{\mathrm{d}\Phi_r(x)}{\mathrm{d}x}\bigg|_L \quad (13)$$

C_p is the capacitance of bimorph; a=1 for parallel and a=2 for series connection of bimorph layers, illustrated by Fig.2; k_r is the coupling term which converts velocity to current; h_{pc} is the distance from the ceramic centerline to neutral axis, and b is the width of the beam. Output voltage and power of bimorph can be identified by simultaneous solving coupling equation (11) and (12),

$$U(t)=\frac{\ddot{y}j\omega k_r\left(-\frac{M_b}{L}\int_0^L\Phi_r(x)dx-M_t\Phi_r(L)\right)}{\left(\frac{a}{2R_L}+\frac{c_p}{a}\right)\left(\omega_r^2-\omega^2+j2\zeta_r\omega_r\omega\right)+j\omega k_r\chi_r} \quad (14)$$

$$P=\frac{U^2}{2R_L} \quad (15)$$

Expression (14) and (15) conclude that output power of bimorph is definitely determined by electromechanical term k_r, for a given input vibration and device size. Therefore, a high piezoelectric constant and low compliance is always desired for high output power.

While anchor is forced to vibrate with external motion, deformation will took place and amplified by tail mass along longitudinal axis, helping to extract charge from piezoelectric film.

The design expects piezoelectric energy harvesting to be utilized in power grid, in which case we have characterized energy output in a vibration-based experiment bench. It's mainly for simulating vibration of power equipments, the predominant frequency of which is 100Hz. Also, the bench is supposed to generate adjustable vibration amplitude in accordance with different vibration intensity. It consists of i) a high power shaker, ii) a controller, iii) a PZT, iv) an oscilloscope, as demonstrated in Fig.21.

(a)

(b)

Fig.21. (a) Setup of vibration-based experiment bench and (b) PZT mounted on fixture of shaker

Dependence of open circuit voltage on frequency is shown in Fig.22. It reveals that PZT is quite sensitive to operational frequency shift from its natural frequency. Taking for example, while operation frequency shifts by 6%, from central 100Hz to 94Hz, open circuit voltage drops 80.1%, from 8.3V to 1.6V. And output scales under each frequency are clearly in positive correlation with motion acceleration.

Fig.23 illustrates load dependence of PZT in resonance status under three accelerations. Load resistance is ranged from 43kΩ to 240kΩ，meanwhile operation voltage applied on load and output power is measured. Output power ascends in the first stage, until it reaches a turning point, then declines. This maximum power point is critical to be identified. It can be tracked by load-matching, keeping R_L=R_{in}. Maximum power of PZT in experiment is 0.08mW, 0.17mW, 0.63mW. PZT is a kind of high impendence devices, and the inner resistance of sample tested is approximately 100kΩ, restricting capability of extracting current from piezoelectric material.

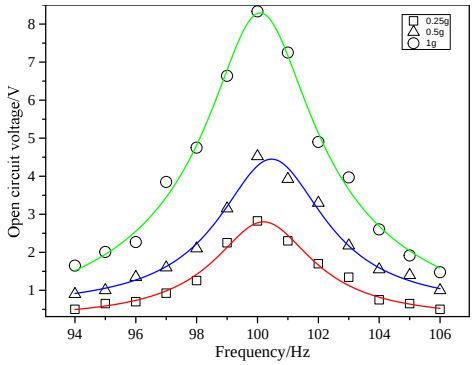

Fig. 22 Frequency dependence of open voltage from PZT

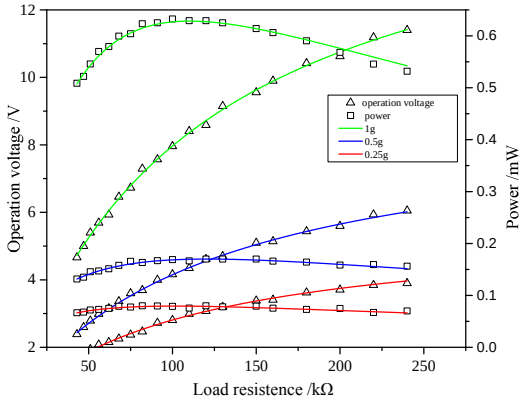

Fig.23 Load dependence of output from PZT in operation

III. HYBRID ENERGY MANAGEMENT SYSEM

A. System Overview

To make recovered energy applicable, it should be regulated before providing a stable electricity to load, usually in the form of certain DC voltage level. However, three kinds of recovered energy have different characteristics. Converted thermoelectric energy corresponds to lower DC voltage level, in order of several dozens of millivolt, meanwhile vibration and magnetic energy are converted into AC voltage with higher level, in order of several volts. It means thermoelectric voltage needs to be stepped up, and vibration and magnetic voltage needs to be rectified and stepped down. Also, due to contradiction on supply-demand between power supply and load consumption, a capacitor or chargeable battery is needed to buffer this power discrepancy.

Another challenge is the low consumption of the energy conditioning system itself, as power loss is unexpected, which is solved by μpower IC technologies. The architecture of hybrid power recovery system is illustrated in Fig.24.

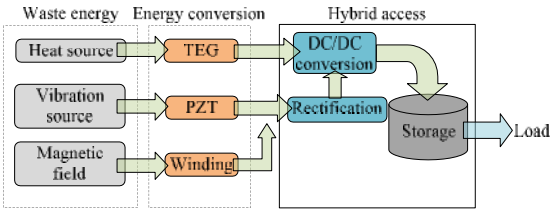

Fig.24. Structure of hybrid power management system

Specially, the above architecture is implemented by IC that integrates rectifiers, boost/bulk modules and controllers, (i.e. LTC 3588, LTC3108). Fig.25 shows the circuit scheme which consists of connectors, LTC 3588, LTC3108, peripheral circuits and storage capacitors. Through not being discussed in this paper, solar energy converted by PV cells still dominants in its output scale. Thus we've considered the possibility of solar energy access if in need and prepared its interface circuit, consisted of LTC 3459 and LTC 2935. The PCB of the system is illustrated in Fig.26.

B. Tentative application

The paper has employed a couple of ZigBee wireless sensors to telemeter temperature as tentative application. They work in 2.4GHz equipped with IEEE 802.15.4 and ZigBee pro. And recovered energy is supposed to power sensor node at least lasting for a life cycle once capacitor has been fully charged. It was observed in test that sensor node reporting data to gateway node every two seconds continually as programmed, without power outrage. This indicates that harvested energy capacity is sufficient for powering sensor node, sustaining voltage across buffer capacitor at valid operational level. It's also supported by the measured waveform of output voltage and load current in Figure 27. Voltage fluctuates from 2V to 2.3V, with ripple coefficient being 14%.

Average current consumption of RF communication

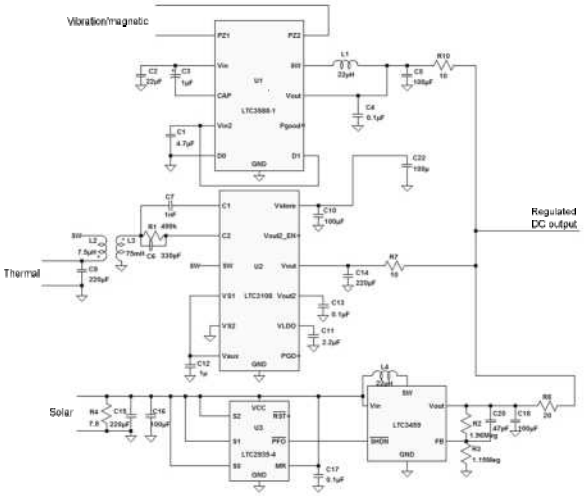

Fig.25 Circuit of hybrid energy management system

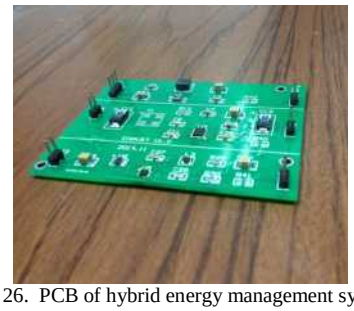

Fig. 26. PCB of hybrid energy management system

is approximately 12mA, calculated from current curve in Fig.27. It means the average power consumption is 25mW. This test demonstrates that overall topology proposed in the paper to recovery magnetic, thermoelectric and vibration energy is feasible and the converted electricity suits the operation of some low-power sensor.

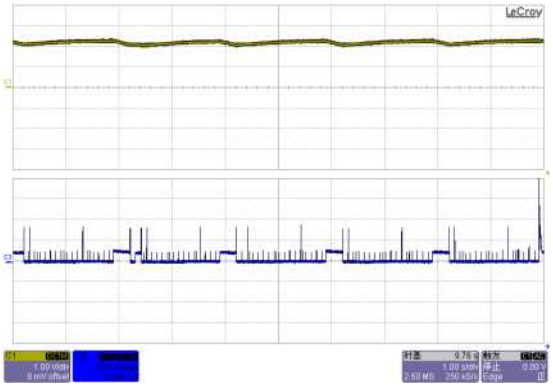

Fig. 27 Waveform of output voltage and load current

IV. ENVISIONED PROTOTYPE

Based on the existing work within the paper, a kind of miniaturized power recovery/harvesting node is presented, see Fig.28. This may be planned as further work. The energy harvested can be used to drive the embedded sensors, data acquisition and wireless communication.

As the topology shows, solar, thermal and vibration modules are incorporated inside the node. They are expected to function independently, consisting highly integrated energy autonomous sensing node. The node can be easily mounted onto any surface if potential energy sources exist.

The design has considered energy conversion, management and power ZigBee sensors. The further work to structure such an envisioned prototype may be more deepgoing structure design to maxim conversion efficiency of multi energy types simultaneously.

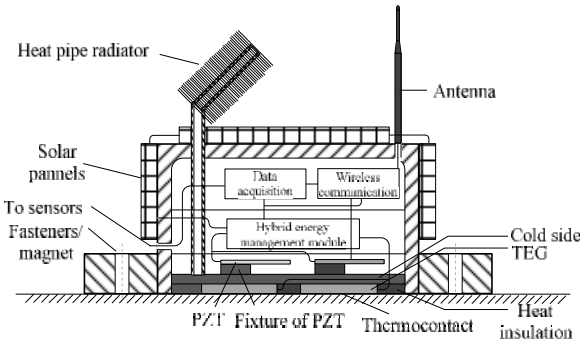

Fig. 28 Envisioned prototype of miniaturized power recovery node.

V. CONCLUSION

Motivated by cosmopolitan problems in energy consumption and the fact of energy waste in power industry, the paper has proposed methods for magnetic, thermoelectric and vibration energy recovery within power grid. Simulation or experiment supports that the three methods and hybrid management system discussed in the paper are suitable for driving low-power sensors using the recovered energy. While solving the problem of power supply for sensors, the work can also give indications for industrial power recovery deployment.

REFERENCES

[1] U.S. Energy Information Administration, International Energy Outlook 2011, DOE/EIA-0484(2011).

[2] Jinxu Ding; Somani, A., "A Long-Term Investment Planning Model for Mixed Energy Infrastructure Integrated with Renewable Energy," Green Technologies Conference, 2010 IEEE , vol., no., pp.1,10, 15-16 April 2010.

[3] Haidar, J.G.; Ghojel, J.I., "Waste heat recovery from the exhaust of low-power diesel engine using thermoelectric generators," Thermoelectrics, 2001. Proceedings ICT 2001. XX International Conference on , vol., no., pp.413,418, 2001.

[4] Cheng Zhou , Qiumin Wu, "The Power Transformer Waste Heat Recovery Feasi-bility Study", Modern Manufacturing Technology and Equipment,vol.,no.,03.,pp.22,29 2012.

[5] Chaoqing Yuan; Sifeng Liu; Benhai Guo, "The relationship among non-fossil energy consumption, economic growth and coal prices in China," Grey Systems and Intelligent Services (GSIS), 2011 IEEE International Conference on , vol., no., pp.339,342, 15-18 Sept. 2011.

[6] Zhu, M.; Baker, P.C.; Roscoe, N.M.; Judd, M.D.; Fitch, J., "Alternative Power Sources for Autonomous Sensors in High Voltage Plant," Electrical Insulation Conference, 2009. EIC 2009. IEEE , vol., no., pp.36,40, May 31 2009-June 3 2009.

[7] Wan, Z.G.; Tan, Y.K.; Yuen, C., "Review on energy harvesting and energy management for sustainable wireless sensor networks," Communication Technology (ICCT), 2011 IEEE 13th International Conference on , vol., no., pp.362,367, 25-28 Sept. 2011.

[8] Roscoe, N.M.; Judd, M.D., "Harvesting Energy From Magnetic Fields to Power Condition Monitoring Sensors," Sensors Journal, IEEE , vol.13, no.6, pp.2263,2270, June 2013.

[9] Typical Design for Power Transmission and Transformation Project of State Grid Corporation: Fascicule of 220kV Substation .

[10] GBJ149—90 Erection Works of Electrical Installations Code for Construction and Acceptance of Bus-bar Device.

[11] Tzu-Chi Huang; Ming-Jhe Du; Yu-Chai Kang; Ruei-Hong Peng; Ke-Horng Chen; Ying-Hsi Lin; Tsung-Yen Tsai; Chao-Cheng Lee; Long-Der Chen; Jui-Lung Chen, "120% Harvesting Energy Improvement by Maximum Power Extracting Control for High Sustainability Magnetic Power Monitoring and Harvesting System," Power Electronics, IEEE Transactions on , vol.30, no.4, pp.2262,2274, April 2015 doi: 10.1109/TPEL.2014.2330868.

[12] Z. J. Chien, H. P. Cho, C. S. Jwo, S. L. Chen, Y. L. Lin, "A Study of Waste-Heat Recovery Unit for Power Transformer", Advanced Materials Research, Vols 875-877, pp. 1661-1665, Feb. 2014.

[13] Dalola, S.; Ferrari, M.; Ferrari, V.; Guizzetti, M.; Marioli, D.; Taroni, A., "Characterization of Thermoelectric Modules for Powering Autonomous Sensors," Instrumentation and Measurement, IEEE Transactions on , vol.58, no.1, pp.99,107, Jan. 2009.

[14] Tan, Y.K.; Panda, S.K., "Energy Harvesting From Hybrid Indoor Ambient Light and Thermal Energy Sources for Enhanced Performance of Wireless Sensor Nodes," Industrial Electronics, IEEE Transactions on , vol.58, no.9, pp.4424,4435, Sept. 2011.

[15] Antonova, E.E.; Looman, D.C., "Finite elements for thermoelectric device analysis in ANSYS," Thermoelectrics, 2005. ICT 2005. 24th International Conference on , vol., no., pp.215,218, 19-23 June 2005.

[16] B. Garcia, J. Burgos, A. Alonso, "Transformer Tank Vibration Modelling as a Method of Detecting winding Deformations-Part II: Experimental Verification", IEEE Tran. On Power Delivery, Vol. 21, No. 1, pp. 164-169, January 2006.

[17] Erturk, D. J. Inman (2009). "An experimentally validated bimorph cantilever model for piezoelectric energy harvesting from base excitations." Smart Mater. and Struct. 18(2): 025009.

Feng Yang received the B.Eng degree in electrical engineering and automation from Chongqing University, Chongqing, China in 2012. He has been working toward the PhD degree in electrical Engineering at Chongqing University since 2012. His research interests include energy harvesting, diagnosis and evaluation of insulation of capacitive power equipments.

Lin Du received the M.S. and Ph.D. degrees in electrical engineering from Chongqing University, Chongqing, China, in 1996 and 2003, respectively. He is currently a Professor with Chongqing University. His major research interests include high-voltage testing technique, online detection of insulation condition of electrical apparatus, insulation fault diagnosis for high-voltage equipments, and online overvoltage monitoring and recognition.